Title: Characterization of polylactide layer deposited on Ni-Ti shape memory alloy

Author: Tomasz Goryczka, Barbara Szaraniec

Citation style: Goryczka Tomasz, Szaraniec Barbara. (2014). Characterization of polylactide layer deposited on Ni-Ti shape memory alloy. "Journal of Materials Engineering and Performance" (Vol. 23, iss. 7 (2014), s. 2682-2686), doi 10.1007/s11665-014-1038-0

JMEPEG (2014) 23:2682–2686
DOI: 10.1007/s11665-014-1038-0

1059-9495/$19.00

Characterization of Polylactide Layer Deposited on Ni-Ti Shape Memory Alloy

Tomasz Goryczka and Barbara Szaraniec

(Submitted February 3, 2014; in revised form April 4, 2014; published online May 16, 2014)

Polylactide (PLA) thin layer was deposited on the surface of the as-quenched NiTi shape memory alloy. First, NiTi alloy was quenched from the 850°C, then its surface was covered with PLA. Deposited PLA is in an amorphous state, whereas the as-quenched NiTi alloy stays in the B2 structure. PLA deposition caused smoothing of the surface and changed its hydrophilic character to hydrophobic one. In general, procedure of PLA deposition does not influence the course of the reversible martensitic transformation. After deformation of NiTi sample covered with PLA up to 4%, its surface does not reveal any cracks and still remains continuous.

Keywords NiTi, polylactide, shape memory alloy, shape memory effect, superelasticity

1. Introduction

The Ni-Ti shape memory alloy is frequently use in medical applications. Number of its practical use for implants and medical devices still grows from year to year (Ref 1, 2). However, in respect to the nickel content there still exists discussion over its biocompatibility and corrosion resistance (Ref 3-7). In order to eliminate any nickel diffusion to a human body as well as limit contact between metallic implant and tissue, the surface of the shape memory alloys can be modified by formation of a protective layer. One of the well-known coatings applied for protection of NiTi surface can be titanium nitrides (Ref 8-10), titanium oxides (Ref 11-13), or diamond-like layers (Ref 14-16). Additionally, surface smoothing reduces adhesion of bacteria as well as a biofilm formation. However, too thick and/or stiff layer can limit or completely block shape memory effect. That is why, biocompatible polymers became at the point of interest when covering of Ni-Ti alloys is considered. One of them can be polylactide (PLA). The PLA is biodegradable polymer with degradation time from 1 to 24 months (dependently on composition) and well metabolized inside of the human body (Ref 17). Using its properties it found application in medicine as material for drug delivery, bone fixing, stitching, etc. (Ref 18). In respect to the degradation time, it can be used as a protection layer for short-time Ni-Ti implants. One of them can be: clamps for bone fracture fixing (healing time shorter than 3 months), cranial reshaping springs (healing time shorter than 6 months), or compression clips for anastomoses (healing time about 1 month), etc. (Ref 19).

In presented work the PLA was used as a protective layer deposited on the surface of NiTi shape memory alloy. Structure of obtained layer, its influence on the course of the martensitic transformation as well as the shape memory effect in the covered alloy was studied.

2. Experimental Data

The commercial NiTi alloy with nominal chemical composition: Ti-50.6 at.% Ni was used as a substrate for PLA deposition. Rectangular samples were cut off, with dimension of 10 mm × 8 mm × 0.8 mm. Before PLA deposition, samples were quenched from 850°C to the iced water. Surface was cleaned in ultrasonic cleaner following by chemical etching in HNO_3 + HF + H_2O solution for 30 s.

In order to cover the NiTi surface, the L-lactide/DL-lactide copolymer 80/20 Purasorb PLA 8038 (PURAC Biochem, The Netherlands) was used. The samples were immersed with a rate of 10 mm/s and dried at room temperature for 24 h. Thickness of the copolymer layers was about 2-3 μm.

Phase identification of the materials was carried out using x-ray diffraction patterns measured in classical Bragg-Brentano geometry in X'Pert Pro diffractometer. Also for the layer characterization x-ray diffraction grazing incident beam technique (GIXD) was applied. All measurements were done at room temperature in 2θ range: 5-140°. Cu $K_{\alpha 1 \text{ and } \alpha 2}$ radiation was used. Pole figures were measured with use of Philips PW 1138 diffractometer equipped with texture goniometer. Pole figures were registered in reflective mode with α angle up to 80°. Calculation of orientation distribution function (ODF) was done with use of LaboTex computer program.

Observation of surface morphology as well as studies of chemical composition was carried out with use of a scanning

This article is an invited paper selected from presentations at the International Conference on Shape Memory and Superelastic Technologies 2013, held May 20-24, 2013, in Prague, Czech Republic, and has been expanded from the original presentation.

Tomasz Goryczka, Institute of Materials Science, Silesian Interdisciplinary Centre for Education and Research, University of Silesia, Chorzow, Poland; and **Barbara Szaraniec**, Department of Biomaterials, AGH University of Science and Technology, Kraków, Poland. Contact e-mails: tomasz.goryczka@us.edu.pl, jozef.lelatko@us.edu.pl, and szaran@agh.edu.pl.

electron microscope (SEM) JEOL JSM 6480 with energy-dispersive x-ray spectroscopy (EDS). Topography of the surface was characterized with use of profilograph Hommel Tester T500, Hommelwerke.

Phase transformation was studied by use of differential scanning calorimeter Mettler Toledo DSC-1 (DSC). Thermograms were measured during sample cooling as well as heating with a rate of 10°C/min at thermal range between −125 and 200°C. Weight of the sample was about 14 mg.

Shape memory effect was studied by means of stress-strain curve measurement. The measurement was done on a testing machine Zwick 7000. Tensile test was performed with a rate of 20 mm/min. Length of the sample was 20 mm.

3. Results and Discussion

3.1 Phase Identification

Figure 1 shows set of the x-ray diffraction patterns registered for the as-quenched NiTi alloy (Fig. 1a), as-received PLA (Fig. 1b), and NiTi alloy after PLA deposition (Fig. 1c).

The x-ray diffraction pattern measured for as-received PLA (before layer deposition) reveals two broaden diffraction peaks which is a proof of the amorphous state of the sample (Fig. 1b). Contrary to that, pattern measured for the NiTi alloy confirmed the presence of the parent phase B2 (Fig. 1a). However, in the measured range there was no evidence of the diffraction line 100_{B2} as well as 200_{B2}. It was caused by the presence of texture. In order to prove that, the $\{100\}_{B2}$, $\{110\}_{B2}$, and $\{211\}_{B2}$ pole figures were measured (Fig. 2). In general, the analyzed texture is not strong. The maximum of the pole density does not exceed five levels. Identification of the crystallographic orientation revealed, that pole density was concentrated around orientation $\{111\}\langle -1\ -1\ 2\rangle$. From ODF calculation it was found that 18% of the grains at the surface was oriented along the identified sheet texture.

In order to verify phase components in the NiTi alloy with deposited PLA layer, the x-ray diffraction patterns were measured with use of the GIXD technique. The measurements were done at the constant alpha angle equals 1°, 0.5°, 0.4°, and 0.3°. An example of obtained result is shown in Fig. 2(c). It can be clearly seen that after deposition PLA still remains amorphous and the NiTi alloy reveals diffraction lines belonging to the B2 parent phase. Decreasing of the alpha angle enables a decrease of the x-ray penetration depth. Going further, it enables determination of the layer sequence as well as

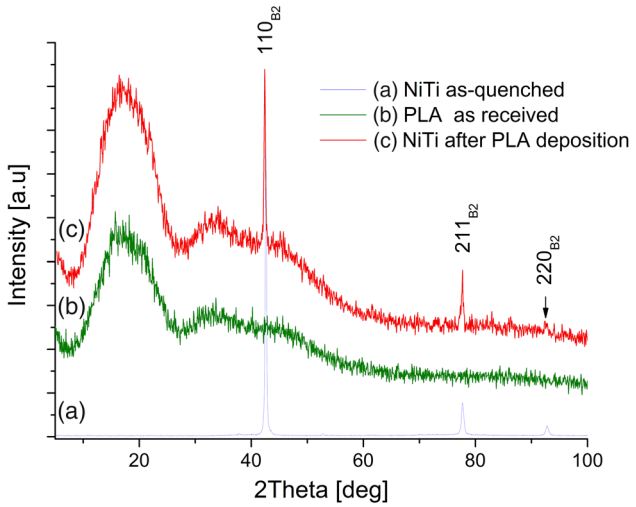

Fig. 1 Set of the x-ray diffraction patterns registered for NiTi alloy (a), PLA (b) and NiTi after the PLA deposition (c)

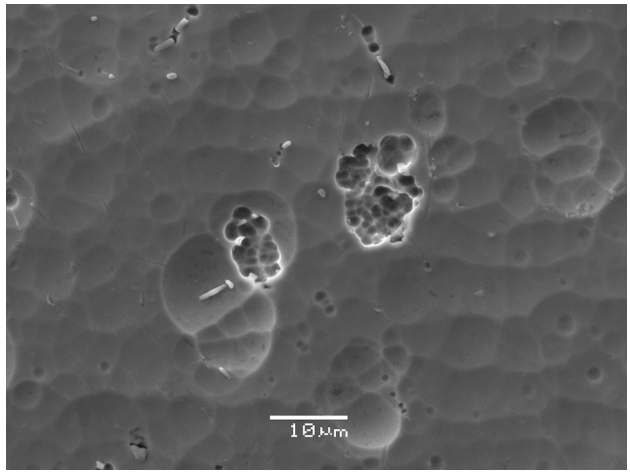

Fig. 3 SEM image observed for surface of as-quenched NiTi alloy after etching

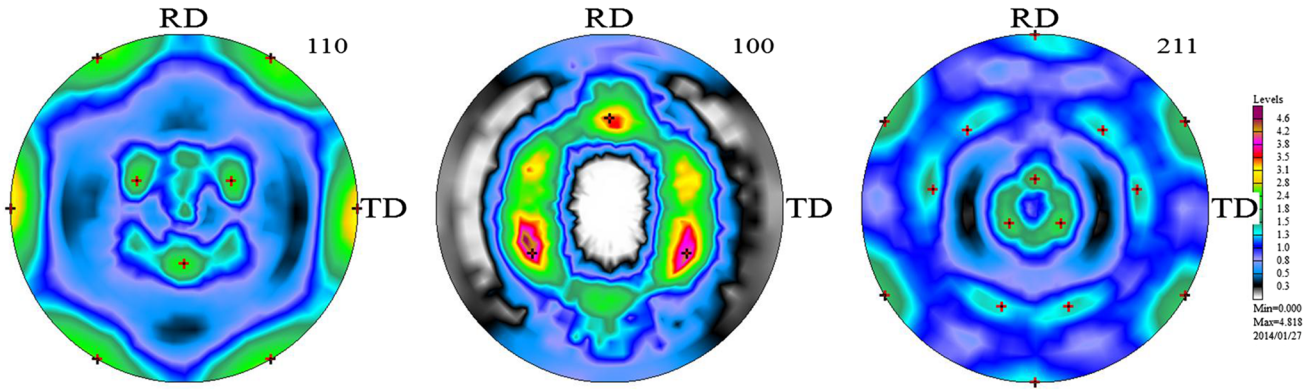

Fig. 2 Pole figures measured for the as-quenched NiTi alloy

phase identification. The decrease of the alpha angle caused lowering of intensities of the B2 phase. Simultaneously, intensities of the broaden peaks belonging to the PLA increased. Such dependence is an evidence that the PLA layer was deposited at the top of the NiTi surface.

3.2 Properties of the Surface

Surface of as-quenched NiTi alloy reveals quite rough character (Fig. 3) as a consequence of the etching applied after quenching. It can be seen that the process caused appearance of craters and pinholes. This procedure enabled for an increase of the contact surface between the alloy and PLA. It is worth noting that at the bottoms of the pinholes as well as in some places at surface, precipitates of the Ti_2Ni phase can be distinguished. The average value of the roughness parameters R_t, R_a, R_z measured for the as-quenched NiTi alloy were: 3.43, 0.51, and 2.8 μm, respectively. After PLA deposition the surface became smoother. The measured parameters were as follows: 1.52, 0.19, and 1.0 μm.

In medical application, wettability of material surface plays an important role. It determines its hydrophobic or hydrophilic character. Figure 4 shows results of the contact angle measurements. At the surface of the as-quenched sample, the drop was spread over a larger area. Value of measured contact angle was 75.1°. It proves hydrophilic character of the as-quenched NiTi alloy. In contrast to that, sample with deposited PLA layer shows a decrease of the contact area of the drop. The contact angle was 117.3°. As regards of that, deposited PLA layer reveals hydrophobic character. In general, the natural PLA shows hydrophilic character with the contact angle varied between 70° and 76° (Ref 20, 21). However, following a technology of the PLA production authors in Ref 21 proved that the PLA can change hydrophilic character to the hydrophobic one.

3.3 Transformation Behavior

In order to study course of the transformations occurring in NiTi alloy as well as in the PLDL copolymer, differential scanning calorimetric analysis was done. Figure 5 shows comparison of the thermograms measured for samples after steps, which were done for surface covering. From thermograms characteristic transformation temperatures (M_s, M_f, M_p, A_s, A_p, A_f, R_s, R_p, R_f) as well as enthalpies were calculated and set in Tables 1 and 2, respectively. As-received NiTi alloy revealed three maxima during cooling and one broaden minimum on heating curve (Fig. 5—blue line). The first maximum, situated at a thermal range between 10 and −10°C on cooling DSC curve, corresponds to the B2 → R-phase transition. Lowering temperature down to −44°C triggers two-stage transformation: the R-phase → B19′. Description of mechanism for two-step transformation occurrence can be found at (Ref 22-24) During heating both transformations B19′ → R-phase and R-phase → B2 overlap at thermal region between −15 and 15°C. From the point of view of the medical application temperatures: R_s (10.4°C) and A_f (14.7°C) are too close to temperature of the human body. In order to lower temperature of the martensitic transformation NiTi alloy was annealed at 850°C for 20 min and quenched into ice-water. First, the thermal treatment changed course of the martensitic transformation. The transition is reversible and occurs in one step B2 ↔ B19′ without any additional presence of the R-phase (Fig. 5—red line). The martensitic transformation starts at −17°C and finishes at −31°C. The reverse transformation starts at about −4°C and finishes at 8°C (Table 1). Also, quenching increased thermal gap between transformation temperatures and temperature of the human body. Also, it increased

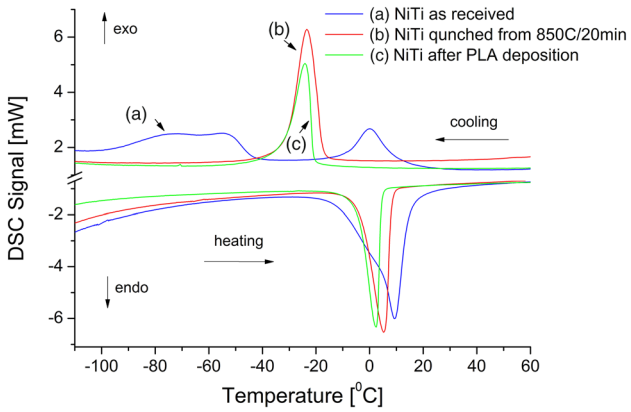

Fig. 5 Thermograms measured for the NiTi alloy before (a, b) and after the PLA layer deposition (c)

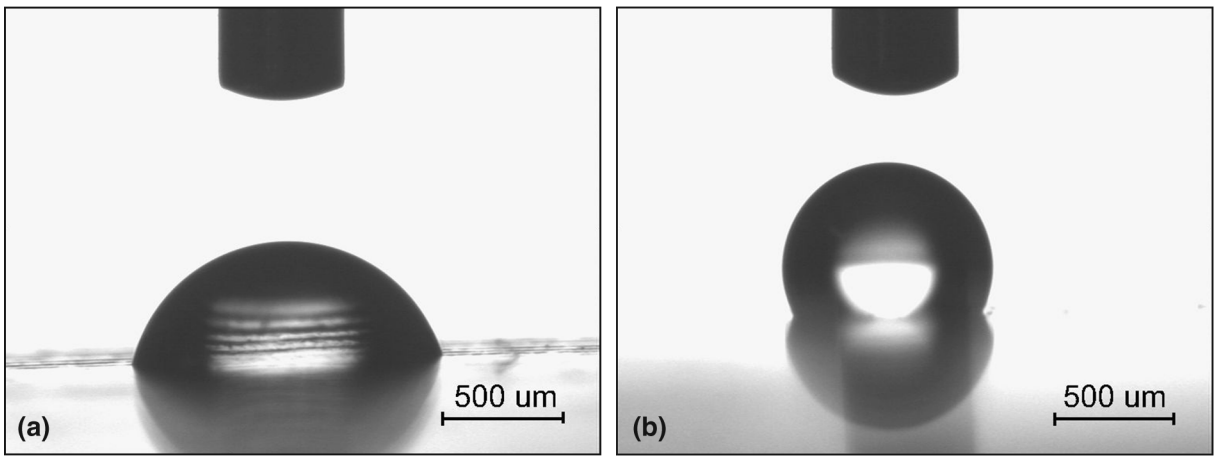

Fig. 4 Shape of the drop spread on surface during contact angle measurement for as-quenched NiTi alloy before (a) and after the PLA deposition (b)

Table 1 Transformation temperatures determined from DSC cooling/heating curves

NiTi alloy	R_s, °C	R_p, °C	R_f, °C	M_s, °C	M_p, °C	M_f, °C	A_s, °C	A_p, °C	A_f, °C
As received	10.4	0.2	−9.7	−43.8	−54.9 −74.2	−96.4	−14.6	9.2	14.7
After quenching	···	···	···	−17.4	−23.4	−31.0	−3.8	5.02	8.12
After PLA deposition	···	···	···	−20.9	−24.1	−32.1	−4.4	2.4	4.5

Table 2 Enthalpy calculated for NiTi alloy before and after PLA deposition

NiTi alloy	$\Delta H^{B2 \rightarrow R}$, J/g	$\Delta H^{R \rightarrow B19}$, J/g	$\Delta H^{B19 \rightarrow B2}$, J/g
As received	3.98	11.08	−15.05
After quenching	···	19.68	−18.97
After PLA deposition	···	14.55	−14.74

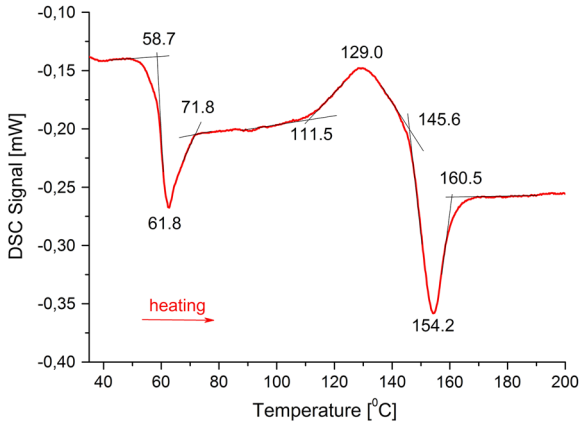

Fig. 6 DSC heating curve measured for the PLA deposited on the NiTi surface

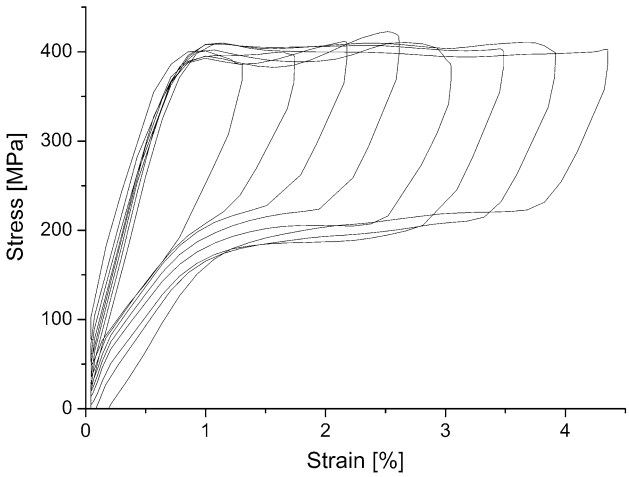

Fig. 7 Shape memory effect in NiTi alloy covered by polylactide layer

transformation enthalpy from 14 up to 19 J/g. After the PLA deposition, thermal behavior of the martensitic transformation remained unchanged. The transformation occurs as a one-step.

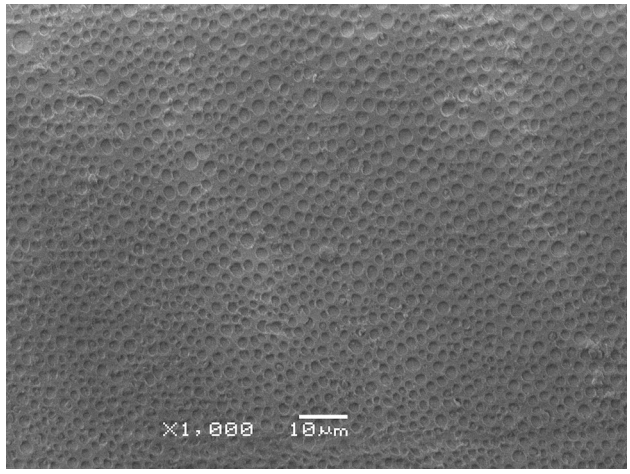

Fig. 8 SEM image observed for NiTi surface with deposition of the PLA layer after sample stretching to 4%

However, its temperatures decreased by about 2°. Also, transformation enthalpy decreased by about 4 J/g. However, this effect was not caused by circumstances of the layer deposition. Lowering of the enthalpy can originate in a lowering of the sample amount, which undergoes martensitic transformation. Weight of the sample was comparable (about 14 mg). However in the covered sample, some amount of the sample was PLA, which does not transform to the martensite as the parent phase B2 does. In comparison to the NiTi alloy, thermal effect of the transformation occurring in the PLA is several times lower. In order to study thermal behavior of the PLA, a part of the layer was removed and separately measured in DSC. Figure 6 shows results of the measurement. Following x-ray diffraction results, the PLA is amorphous at room temperature (Fig. 2). During the PLA heating, the polymer undergoes three transitions. First, the glass transition starts at about 59°C and goes with the highest speed at 62°C. It is followed by crystallization, which occurs at 129°C with enthalpy 6.8 J/g. Finally PLA melts at 154°C (enthalpy −8.9 J/g). Obtained values of the temperature transition are in a good agreement with ones given in Ref 25. It is worth noticing, that thermal behavior of the as-quenched NiTi alloy as well as deposited the PLA, shows ±30°C distance from the temperature of the human body.

3.4 Shape Memory Effect

The response of the covered NiTi alloy for applying external stress was studied by a cyclic axial loading and unloading up to 4.5% elongation of the sample. The covered NiTi alloy reveals typical behavior observed in the shape memory alloys with the superelastic phenomena (Fig. 7). First, the sample undergoes elastic response for the stress. Exceeding value of the critical

stress (about 400 MPa) causes start of the forward martensitic transformation. The evidence of that is almost constant value of the stress when strain increases. Initially, unloading of the sample is elastic up to 200 MPa. Further unloading causes appearance the other plateau, which is related to the reverse martensitic transformation occurrence. During strain decreasing, with the almost constant stress, the martensite is transformed to the parent phase. After unloading, sample came back to the original dimension. Observation of the surface, done for the strengthen sample, showed that PLA surface did not reveal any cracks (Fig. 8). Moreover, PLA layer was elastic enough, that it followed NiTi alloy stretching and did not limit shape memory effect. Following mechanical properties of the PLA, it can stand up elongation up to 6%.

4. Conclusions

- L-Lactide/DL-Lactide copolymer deposited on the NiTi surface changed its character from the hydrophilic to hydrophobic.
- Deposited PLA layer with thickness of 2-3 μm, follows elongation, caused by shape memory effect, up to 4% keeping continuous surface without any cracks.
- The presence of PLA coatings on NiTi alloy does not influence on temperature of martensitic transformation and shape memory effect.
- The PLA coatings can be useful way for NiTi surface protection, when it is applied in medicine for short-time implants.

References

1. T. Yoneyama and S. Miyazaki, *Shape Memory Alloys for Biomedical Applications*, Woodhead, Cambridge, 2008
2. D.L. Yahia, *Shape Memory Implants*, Springer, Berlin, 2000
3. S.S. Shablovskaya, On the Nature of the Biocompatibility and on Medical Applications of NiTi Shape Memory and Superelastic Alloys, *Biomed. Mater. Eng.*, 1996, **6**, p 267–289
4. H. Sigel and A. Sigel, *Metal Ions in Biological Systems: Nickel and Its Role in Biology,*, Vol 23, Mercel Deccer, New York, NY, 1988
5. A.A. Karaczyn, F. Golebiowski, and K.S. Kasprzak, Ni(II) Affects Ubiquitination of Core Histones H2B and H2A, *Exp. Cell Res.*, 2006, **312**, p 3252–3259
6. H. Sigel and A. Sigel, *Nickel and Its Role in Biology*, Mercel Deccer, New York, NY, 1988
7. M. Dinescu, V.C. Dinca, S. Soare, A. Barbalat, C.Z. Dinu, A. Moldovan, and V.F. De Stefano, Nickel Titanium Alloy: Cytotoxicity Evaluation on Microorganism Culture, *Appl. Surf. Sci.*, 2006, **252**, p 4619–4624
8. D. Starosvetsky and I. Gotman, Corrosion Behavior of Titanium Nitride Coated Ni-Ti Shape Memory Surgical Alloy, *Biomaterials*, 2001, **22**, p 1853–1859
9. J. Lelątko, P. Pączkowski, T. Goryczka, T. Wierzchoń, Z. Paszenda, and H. Morawiec, Surface Structure and Corrosion Resistivity of the Nitrided NiTi Alloys, *Eng. Biomater.*, 2005, **247–253**, p 133–138
10. Y. Cheng and Y.F. Zheng, Deposition of TiN Coatings on Shape Memory NiTi Alloy by Plasma Immersion Ion Implantation and Deposition, *Thin Solid Films*, 2006, **515**, p 1358–1363
11. H. Morawiec, T. Goryczka, J. Lelątko, Z. Lekston, A. Winiarski, E. Rówiński, and G. Stergioudis, Surface Structure of NiTi Alloy Passivated by Autoclaving, *Mater. Sci. Forum*, 2010, **636–637**, p 971–976
12. C.L. Chu, S.K. Wu, and Y.C. Yen, Oxidation Behavior of Equiatomic NiTi Alloy in High Temperature Air Environment, *Mater. Sci. Eng. A*, 1996, **216**, p 193–200
13. S.G. Firstov, R.G. Vitchev, H. Kumar, B. Blanpain, and J. Van Humbeeck, Surface Oxidation of NiTi Shape Memory Alloy, *Biomaterials*, 2002, **23**, p 4863–4871
14. J.H. Sui and W. Cai, Effect of Diamond-Like Carbon (DLC) on the Properties of the NiTi Alloys, *Diamond Relat. Mater*, 2006, **15**, p 1720–1726
15. R. Hang and Y. Qi, A Study of Biotribological Behavior of DLC Coatings and Its Influence to Human Serum Albumin, *Diamond Relat. Mater.*, 2010, **19**, p 62–66
16. J.S. Sui, W. Cai, and L. Zhao, Surface Modification of NiTi alloys Using Diamond-Like Carbon (DLC) Fabricated by Plasma Immersion Implantation and Deposition (PIIID), *Nucl. Instr. Methods Phys. Res. B*, 2006, **248**, p 67–70
17. Y. You, B.M. Min, S.J. Lee, T.S. Lee, and W.H. Park, In Vitro Degradation Behavior of Electrospun Polyglycolide, Polylactide, and Poly(lactide-co-glycolide), *J. Appl. Polym. Sci.*, 2005, **95**, p 193–200
18. L.T. Sin, A.R. Rahmat, and W.A.W.A. Rahman, *Polylactic Acid: PLA Biopolymer Technology and Applications*, William Andrew, Oxford, 2012
19. Z. Lekston, T. Goryczka, and H. Morawiec, NiTi Shape Memory Implants Applied in Clinical Studies, *Eng. Biomater.*, 2011, **109–111**, p 62–65
20. J. Zhang, J. Kang, X. Zhang, and H. Zhou, Change of Chemical Bond and Wettability of Polylacticacid Implanted with High-Flux Carbon Ion, *Mater. Sci. Eng. B*, 2008, **151**, p 169–173
21. H.-C. Chen, C.-H. Tsai, and M.-C. Yang, Mechanical Properties and Biocompatibility of Electrospun Polylactide/poly(vinylidene fluoride) Mats, *J. Polym. Res.*, 2011, **18**, p 319–327
22. H. Morawiec, D. Stróż, T. Goryczka, and D. Chrobak, Two-Stage Martensitic Transformation in a Deformed and Annealed NiTi Alloy, *Scr. Mater.*, 1996, **35**, p 485–490
23. J. Khalil-Allafi, G. Eggeler, A. Dlouhy, W.W. Schmahl, and Ch Somsen, On the Influence of Heterogeneous Precipitation on Martensitic Transformations in a Ni-rich NiTi Shape Memory Alloy, *Mater. Sci. Eng. A*, 2004, **378**, p 148–151
24. D. Chrobak, D. Stróż, and H. Morawiec, Effect of Early Stages of Precipitation and Recovery on the Multi-Step Transformation in Deformed and Annealed Near-Equiatomic NiTi Alloy, *Scr. Mater.*, 2003, **48**, p 571–576
25. A.J.R. Lasprilla, G.A.R. Martinez, and B. Hoss, Synthesis and Characterization of Poly(lactic acid) for Use in Biomedical Field, *Chem. Eng.*, 2011, **24**, p 985–990